Wind-driven river plume dynamics and toxic *Alexandrium tamarense* blooms in the St. Lawrence estuary (Canada): A modeling study

Juliette Fauchot [a,b,1], François J. Saucier [a], Maurice Levasseur [c,*], Suzanne Roy [a], Bruno Zakardjian [a]

[a] *Institut des Sciences de la Mer de Rimouski (ISMER), Université du Québec à Rimouski, Rimouski, Québec, Canada G5L 1C9*
[b] *Maurice Lamontagne Institute, Fisheries and Oceans Canada, Mont-Joli, Québec, Canada G5H 3Z4*
[c] *Université Laval, Département de Biologie, Pavillon Alexandre-Vachon, Ste-Foy, Québec, Canada G1K 7P4*

Abstract

In the lower St. Lawrence estuary (LSLE, eastern Canada), blooms of the toxic dinoflagellate *Alexandrium tamarense* are a recurrent phenomenon, resulting in paralytic shellfish poisoning outbreaks every summer. A first coupled physical–biological model of *A. tamarense* blooms was developed for this system in order to explore the interactions between cyst germination, cellular growth and water circulation and to identify the effect of physical processes on bloom development and transport across the estuary. The simulated summer (1998) was characterized by an *A. tamarense* red tide with concentrations reaching 2.3×10^6 cells L^{-1} along the south shore of the LSLE. The biological model was built with previously observed *A. tamarense* cyst distribution, cyst germination rate and timing, and *A. tamarense* growth limitation by temperature and salinity. The coupled model successfully reproduced the timing of the *A. tamarense* bloom in 1998, its coincidence with the combined plumes from the Manicouagan and Aux-Outardes (M-O) rivers on the north shore of the estuary, and the temporal variations in the north-south gradients in cell concentrations. The simulation results reveal that the interaction between cyst germination and the estuarine circulation generates a preferential inoculation of the surface waters of the M-O river plume with newly germinated cells which could partly explain the coincidence of the blooms with the freshwater plume. Furthermore, the results suggest that the spatio-temporal evolution of the bloom is dominated by alternating periods of retention and advection of the M-O plume: east or north-east winds favor the retention of the plume close to the north shore while west or north-west winds result in its advection toward the south shore. The response of the simulated freshwater plume to fluctuating wind forcing controls the delivery of the *A. tamarense* bloom from the northern part of the estuary to the south shore. In addition, our results suggest that a long residence time of the M-O plume and associated *A. tamarense* population in the LSLE during the summer 1998 contributed to the development of the red tide. We thus hypothesize that the wind-driven dynamics of the M-O plume could partly determine the success of *A. tamarense* blooms in the LSLE by influencing the residence time of the blooms and water column stability, which in turn affects *A. tamarense* vertical migrations and growth.

* Corresponding author. Tel.: +1 418 656 2131x3207; fax: +1 418 656 2339.
  E-mail address: Maurice.Levasseur@bio.ulaval.ca (M. Levasseur).
[1] Present address: IFREMER, DYNECO, Centre de Brest, B.P. 70, 29280 Plouzané, France.

1. Introduction

Harmful algal blooms represent a serious and widespread threat to marine ecosystems, fisheries resources and human health. There is, therefore, a need to understand better the population dynamics of the responsible species and to develop our capability to predict and manage these harmful blooms. Several studies have thus attempted to identify the ecological and oceanographic factors influencing the development of these blooms, with a particular attention to the key physical–biological interactions involved.

In the lower St. Lawrence estuary (eastern Canada), blooms of the dinoflagellate *Alexandrium tamarense* are a recurrent phenomenon, causing major outbreaks of paralytic shellfish poisoning (Blasco et al., 2003). *A. tamarense* presents a complex life cycle with a dormant phase in the sediments and a vegetative phase in the water column. After a period of dormancy, the sedimentary cysts germinate into vegetative cells that migrate to surface waters and can potentially initiate a new bloom. In the lower St. Lawrence estuary (LSLE), Cembella et al. (1988) and Turgeon et al. (1990) reported very high concentrations of *A. tamarense* cysts in the sediments along the north and south coasts. A few years later, Perez et al. (1998) showed that the germination rate of these *A. tamarense* cysts was constant at ca. 20% all year round, except for a strong increase in germination in late summer/early fall. During the vegetative growth season, the blooms are mostly confined to the plume formed by the Manicouagan and Aux-Outardes (M-O) rivers located on the north shore of the estuary (Therriault et al., 1985; Cembella and Therriault, 1989). Such coincidence between *Alexandrium* blooms and freshwater plumes has been previously reported in the Gulf of Maine (Franks and Anderson, 1992; Anderson et al., 2005). The cause for the presence of *A. tamarense* in the M-O freshwater plume in the LSLE has not yet been identified, although a positive effect of stratification is suspected (Therriault et al., 1985; Cembella and Therriault, 1989). Recently, Fauchot et al. (2005a) found that *A. tamarense in situ* growth rates could vary between 0.20 and 0.55 day^{-1} in the LSLE, but that significant growth only occurred in the river plumes at salinity below 24.5. These results indicate a tight interaction between the hydrodynamical conditions and the biological characteristics of *A. tamarense* cells.

The objective of this work was to develop a first physical–biological model of *A. tamarense* for the lower St. Lawrence estuary and to use this model to explore the impact of interactions between cyst germination of *A. tamarense*, cellular growth and water circulation on the accumulation and transport of *A. tamarense* cells. The study focuses on the initiation and development period of a red tide, which occurred in July 1998 in the LSLE.

2. Material and methods

2.1. The lower St. Lawrence estuary

The lower St. Lawrence estuary is a large-scale estuary (30–50 km wide, Fig. 1) and its major bathymetric feature is the Laurentian channel with depths exceeding 300 m (e.g., Ingram and El-Sabh, 1990). The mesoscale water circulation, strongly influenced by Coriolis effects, is complex and exhibits important spatial and temporal variability (e.g., Ingram and El-Sabh, 1990; Vézina et al., 1995). The mean hydrodynamic conditions in the LSLE are driven by the fresh-water runoff from the St. Lawrence, Saguenay, Bersimis, Manicouagan and Aux-Outardes rivers and strong tidal forcing (Koutitonsky and Bugden, 1991). However, deviations from a classic estuarine circulation pattern have been reported and are associated to the dynamics of wide straits, e.g., cross-channel currents and fresh waters flowing seaward along the north shore (Ingram and El-Sabh, 1990; Koutitonsky et al., 1990). In April–May, the freshwater runoff induces a large decrease in the mean surface salinity of the estuary and the establishment of a strong stratification that persists until fall (Therriault and Levasseur, 1986).

2.2. The three-dimensional circulation model

A detailed description of the coastal sea ice-ocean coupled model is presented in Saucier et al. (2003, 2004). The model domain covers the estuary and the gulf of St. Lawrence bounded by Cabot Strait, the Strait of Belle-Isle, and the upper limit of the tidal influence near Ile d'Orleans (Fig. 1). The ocean model solves the hydrostatic shallow water equations with a finite difference scheme, and incorporates a level 2.5 turbulent closure scheme. A dynamic (Hunke and Dukowicz, 1997) and two layer thermodynamic (Semtner, 1976) sea ice model is coupled with the ocean model. Bulk aerodynamic exchange formulae govern the heat fluxes between the ocean, sea ice and atmosphere. The grid resolution is 5 km on the horizontal and ranges from 5 to 20 m in the vertical, with free surface and bottom layers adjusted to topography. The model is deterministic only and tracer conserving, driven by detailed atmospheric
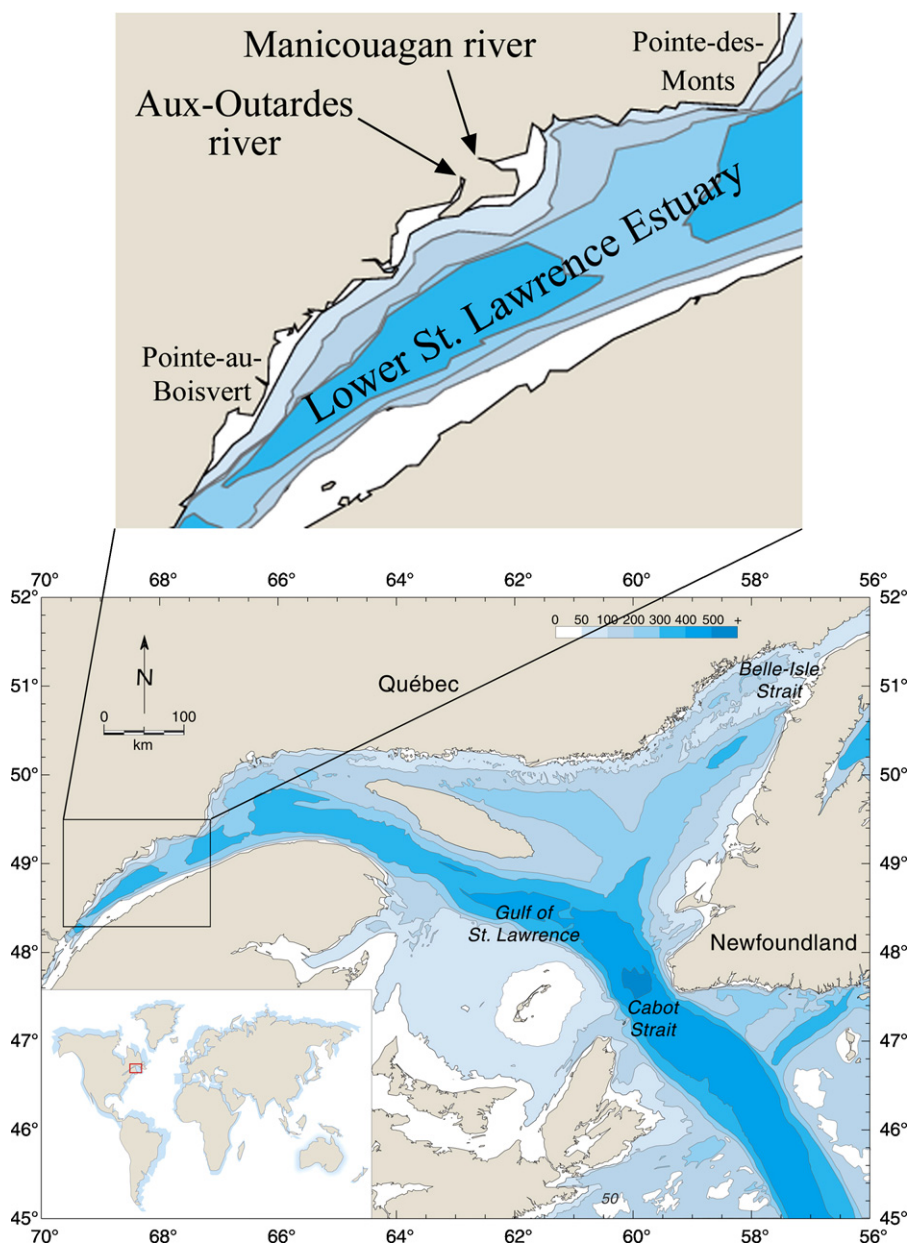
Fig. 1. Map of the estuary and the gulf of St. Lawrence showing the model domain and the sub-region of the lower St. Lawrence estuary concerned by the present study. Modified from the St. Lawrence observatory web site (www.osl.gc.ca).

forcings (3-hourly winds, short and long wave radiation, precipitation), daily river runoffs from the St. Lawrence river and the 28 most important tributaries, hourly water levels (co-oscillating tides), and climatological mean temperature and salinity profiles at the Strait of Belle-Isle and Cabot Strait. Simulations for 1996–1997 (Saucier et al., 2003) and subsequent years until 2003 (Le Fouest et al., 2006; Smith et al., submitted for publication) have been successfully compared to observed temperature and salinity, sea ice cover, water

levels, and past analyses of transport in the lower estuary and gulf. Initial temperature and salinity conditions are provided from a synoptic survey carried during November 1997.

2.3. The biological model of A. tamarense bloom development

The model was developed for the LSLE region, from Pointe-au-Boisvert to Pointe des Monts (Fig. 1). The

germination was implicitly simulated by adding germinated cells in the deepest layer of the model at each time step. This input of newly germinated cells was calculated from the observed cyst distribution previously reported (Cembella et al., 1988; Turgeon et al., 1990) and from laboratory measurements of germination rate (Perez et al., 1998). As reported by Perez et al. (1998), the germination rate used for the calculation was constant during the simulation period (20% per month from April to August). The newly germinated cells swim upward at $1 \, \text{m} \, \text{h}^{-1}$ until they reach the surface layer of the model (0–5 m) where they become vegetative cells. These vegetative cells (modeled as passive Eulerian tracers) grow only in the first three layers of the model (0–15 m depth range), with a temperature and salinity dependent growth rate. The circulation model tends to generate temperatures and salinities slightly higher and lower, respectively, than *in situ* during the studied period. To take into account these differences, the temperature and salinity thresholds for the limitation of *A. tamarense* growth in the biological model were adjusted as follows: 2 °C were added to the temperature threshold and 2 units were subtracted from the salinity threshold. Thus, below a temperature of 9 °C (7 °C in Prakash, 1967) and above a salinity of 22.5 (24.5 according to Fauchot et al., 2005a), the growth rate of the vegetative cells in the first three layers of the model is inhibited and their mortality rate is set at 0.05 day^{-1}. Above a temperature of 9 °C and below a salinity of 22.5, the mortality rate is null and the growth rate is 0.3 day^{-1}, according to growth rates previously measured in the laboratory and in the field for *A. tamarense* strains from the St. Lawrence estuary (Levasseur et al., 1995; MacIntyre et al., 1997; Parkhill and Cembella, 1999; Fauchot et al., 2005a).

The biological model was coupled with the physical model by introducing the following field equation for an active Eulerian tracer that is transported and diffused in the simulated 3D currents:

$$\frac{\partial C}{\partial t} + \nabla(VC) - K_h \nabla_h^2 C - \frac{\partial}{\partial z}\left(K \frac{\partial C}{\partial z}\right)$$
$$= -\frac{\partial w_z C}{\partial z} + \text{sources} - \text{sinks} \tag{1}$$

where C is the newly germinated cell or the vegetative cell concentration, V the current (with three components: u, v, w), K_h and K are respectively the horizontal and vertical diffusion coefficient and w_z is the vertical swimming speed for the newly germinated cells only. The simulation with the biological model coupled to the three-dimensional circulation model was run from 1st

December 1997 to 30 August 1998, although cyst germination in the biological model only begins on 1st April. The results presented are daily averaged model outputs.

2.4. Field measurements for model validation

The *A. tamarense* bloom was followed at two coastal monitoring stations in the LSLE during the summer 1998: Baie-Comeau on the north shore and Sainte-Flavie on the south shore. Surface water samples were collected with a bucket once a week. The sampling took place at high tide and during daylight hours (see Blasco et al., 2003 for details on the monitoring program). On each sampling day, water temperature and salinity were measured and water samples were collected for *A. tamarense* enumeration. When the *A. tamarense* bloom was detected at the monitoring station of Sainte-Flavie, the sampling frequency was increased from weekly to daily.

At the peak of the observed *A. tamarense* bloom, on 8 and 9 July 1998, additional stations were sampled by helicopter. Surface water samples were collected using a Niskin bottle lowered from the heplicopter. Another helicopter survey was conducted on July 12. At each station, surface water temperature and salinity were measured and water samples were taken for *A. tamarense* enumeration. Finally, sampling along a south-north transect across the estuary was conducted on July 13 on the C.C.G.S. Martha L. Black. During this cruise, water samples were collected for the identification and enumeration of *A. tamarense* at 2 m using a rosette equipped with Niskin bottles. A detailed description of the sampling, the measurements of salinity and temperature and *A. tamarense* enumeration during the summer 1998 is presented in Fauchot et al. (2005a).

3. Results

3.1. Influence of the interaction between cyst germination and the estuarine circulation on the simulated inoculation of surface waters with A. tamarense vegetative cells

The biological model simulation began on 1st April with *A. tamarense* cyst germination. However, due to temperature limitation of growth (temperature <9 °C, Fig. 2a), *A. tamarense* cells did not grow until 13 May. The cell distribution generated by the coupled model when germination took place in absence of cellular growth represents the period of initiation of the bloom.
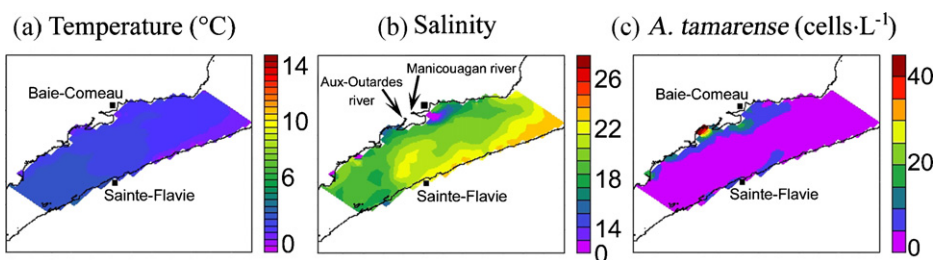
Fig. 2. Simulated daily mean temperature (a), salinity (b) and cell concentration (c) in the surface layer of the model (0–5 m) during the initiation of the bloom, on 15 April 1998. The location of the Manicouagan and Aux-Outardes rivers is indicated in b.

The distribution of *A. tamarense* cells during this initiation period is shown in Fig. 2. The interaction between cyst germination and the estuarine circulation during the simulation generated a higher, and almost exclusive, inoculation of the surface waters along the north shore (Fig. 2c). Very few cells were found on the south shore, even if cyst concentrations and the germination rate in the biological model were similar
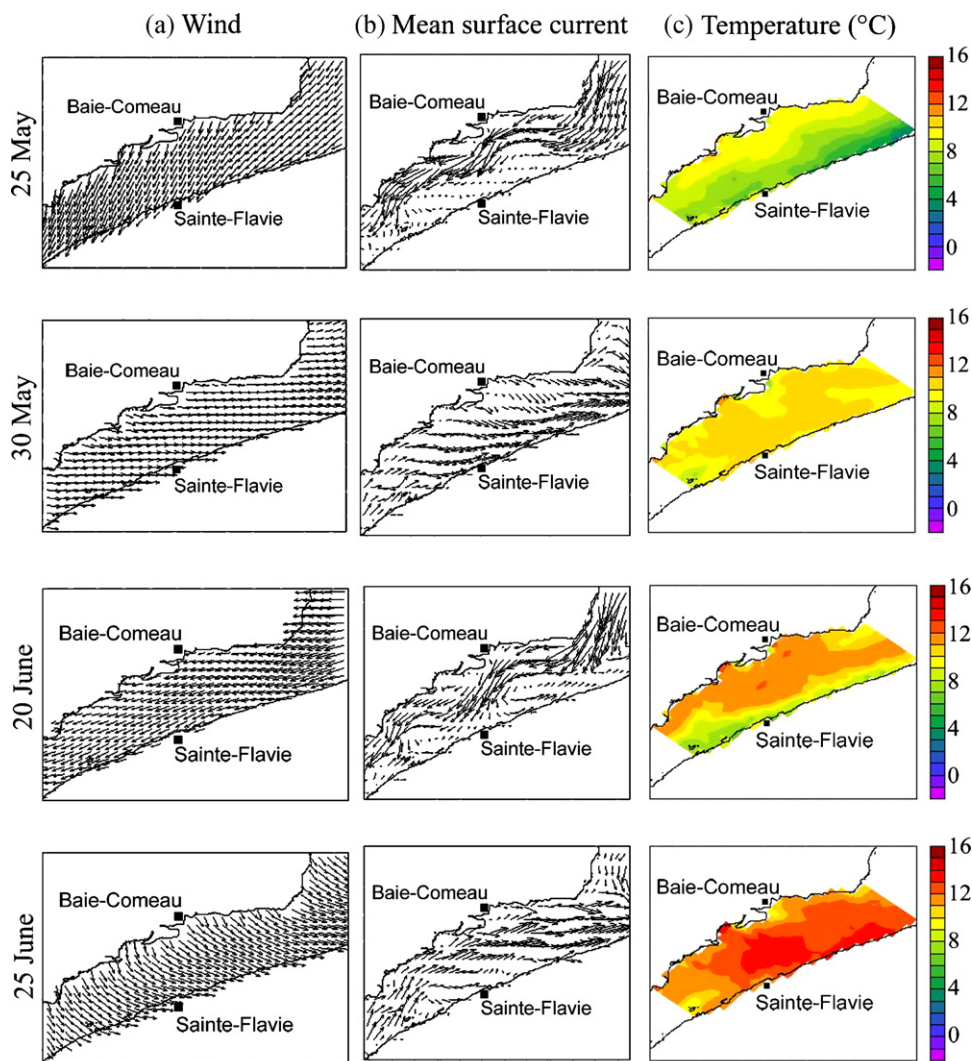

Fig. 3. Daily mean wind (a), simulated currents (b), temperature (c), salinity (d), *A. tamarense* growth rate (e) and cell concentration (f) in the surface layer of the model (0–5 m), during two episodes of retention (25 May and 20 June) and advection (30 May and 25 June) of the M-O freshwater plume. The location of the transect illustrated in Fig. 4 is indicated in f.
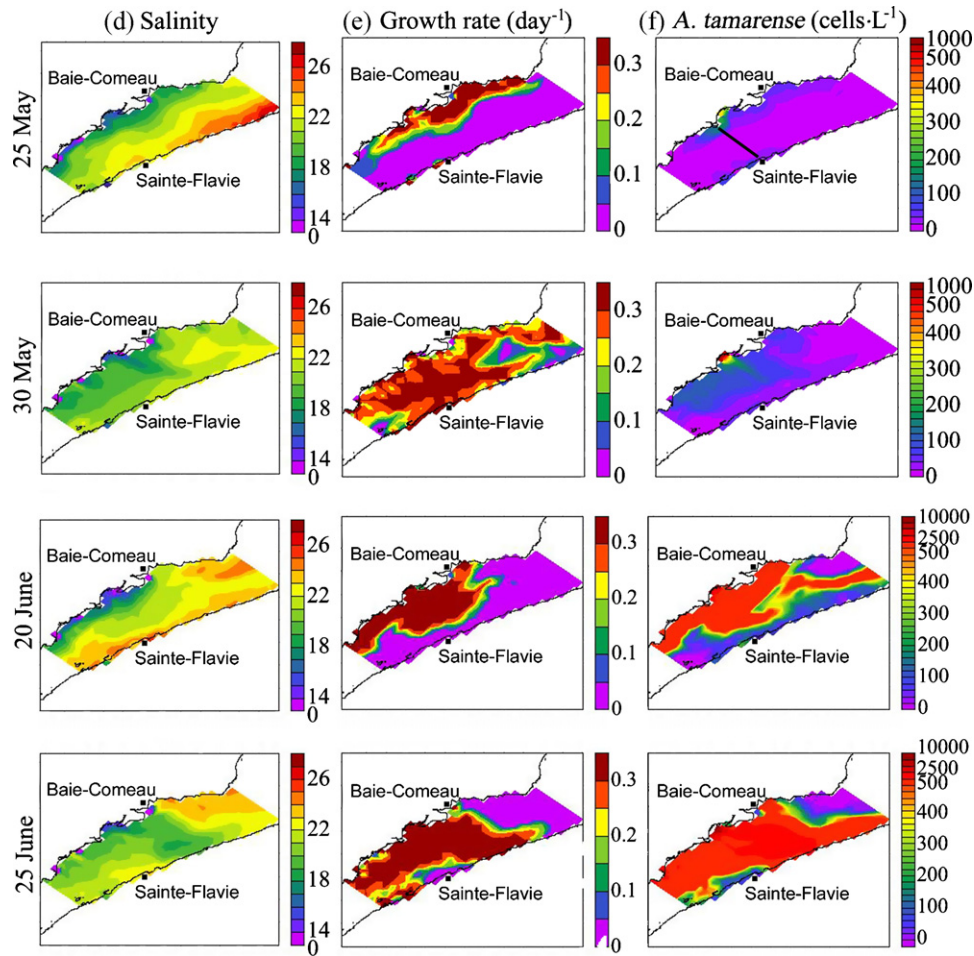
Fig. 3. (*Continued*).

along both shores of the estuary. The simulated preferential inoculation along the north shore took place especially in the region of the combined freshwater plumes of the M-O rivers (Fig. 2b and c).

3.2. Influence of the Manicouagan and Aux-Outardes (M-O) freshwater plume dynamics on the A. tamarense bloom

From 13 May on, the simulated warming of the surface water allowed the growth of *A. tamarense* vegetative cells (Fig. 3c). Due to growth rate limitation by salinity, the simulated *A. tamarense* growth was restricted to freshwater plumes, especially to the M-O plume (Fig. 3d and e). The model generated an *A. tamarense* bloom that developed mainly in this plume (Fig. 3f). The results of the simulation reveal a succession of periods of retention and of advection of the M-O plume during the summer 1998. During

simulated periods of retention, the plume remained close to the north shore (e.g., 25 May and 20 June, Fig. 3d). In contrast, during simulated periods of advection, the surface waters of the freshwater plume extended toward the south shore (e.g., 30 May and 25 June, Fig. 3d). The simulation results show that the distribution of *A. tamarense* cells is closely associated with the dynamics of the M-O plume: during periods of advection, the cells were transported toward the south shore with the freshwater plume (Fig. 3f). This process is clearly illustrated by the vertical profiles of simulated temperature, salinity and *A. tamarense* cell concentrations presented in Fig. 4. During the period of retention (Fig. 4a–c), the simulated bloom developed in, and was almost completely restricted to the freshwater plume close to the north shore. Then, during the period of advection (Fig. 4d–f), the M-O plume thinned while extending to the south and the *A. tamarense* patch spread toward the south shore with the plume. The
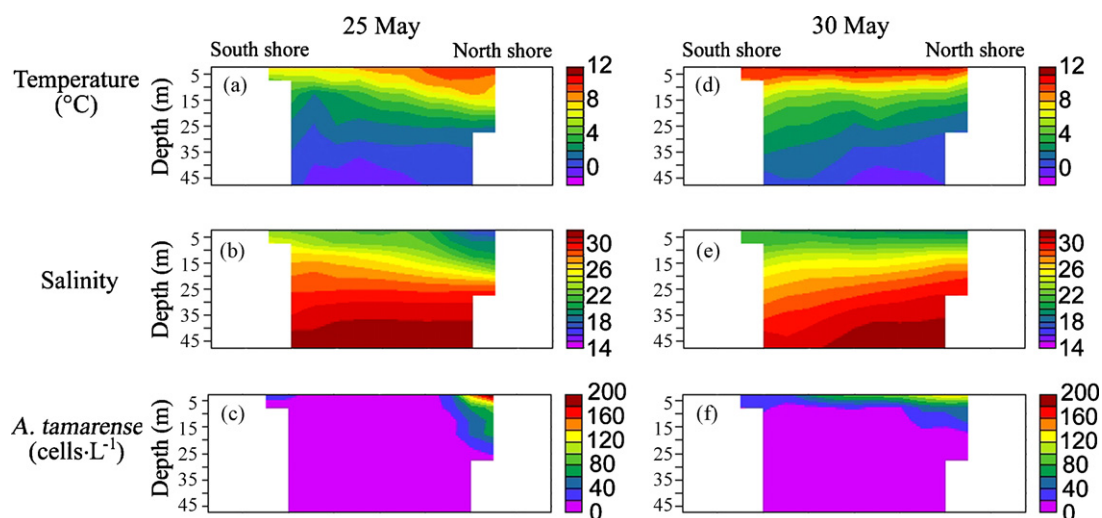
Fig. 4. Vertical profiles of simulated daily mean temperature (a and d), salinity (b and e) and *A. tamarense* cell concentration (c and f) on 25 May (episode of retention) and 30 May (episode of advection toward the south shore). The location of the transect is indicated in Fig. 3.

variations in the north-south extent of the M-O plume simulated by the model were mainly the result of wind stresses on the circulation of surface waters in the LSLE. Under easterly or northeasterly winds (Fig. 3a, 25 May and 20 June), the model generated upstream currents in the surface layer of the northern part of the estuary (Fig. 3b), resulting in the retention of the M-O

freshwater plume close to the north shore. Under westerly or northwesterly winds (Fig. 3a, 30 May and 25 June), the model generated downstream and southward cross-channel surface currents (Fig. 3b), resulting in the advection of the M-O plume toward the south shore. The delivery to the south shore of the simulated bloom appears to depend, therefore, on the wind-driven
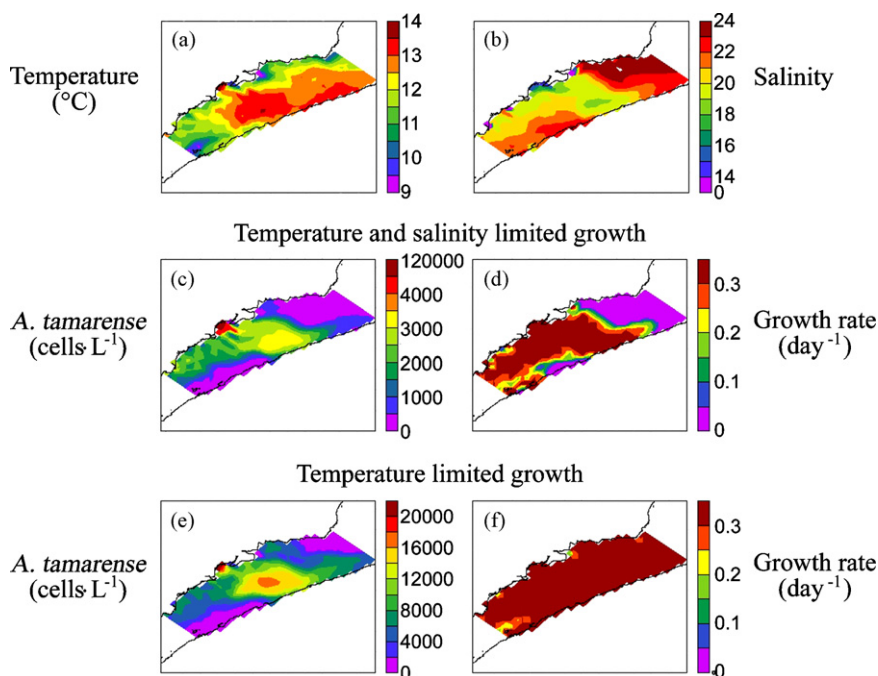

Fig. 5. Simulated daily mean temperature (a) and salinity (b), *A. tamarense* cell concentration (c and e) and growth rate (d and f) in the surface layer of the model (0–5 m) on 25 June, with and without the salinity limitation of growth.

retention–advection cycles of the M-O plume. Furthermore, the simulation results suggest that the retention of surface waters in the LSLE was important during the summer 1998, since the total duration of retention periods (35 days) was more important than the advection periods (32 days) during the development of the bloom (1st May to 20 July).

3.3. Effect of the simulated salinity limitation of A. tamarense growth on bloom distribution

The results of the simulation confirm previous field observations showing that *A. tamarense* blooms are tightly associated with the M-O freshwater plume. In order to determine if the association between *A. tamarense* blooms and the M-O freshwater plume

resulted from growth rate limitation at high salinity, we ran a simulation where *A. tamarense* growth rate was only limited by temperature (no salinity constraint on growth). For that run, cell growth rate was thus not restricted to the freshwater plume (Fig. 5f). Removing the salinity limitation of *A. tamarense* growth did not affect its distribution (Fig. 5c and e). Thus, the simulated association between the *A. tamarense* bloom and the freshwater plume did not result from the inhibition of growth in higher salinity surface waters.

3.4. Model results versus observations

Comparison of the temporal evolution of the bloom between the results of the simulation and the observations at two monitoring stations during the summer
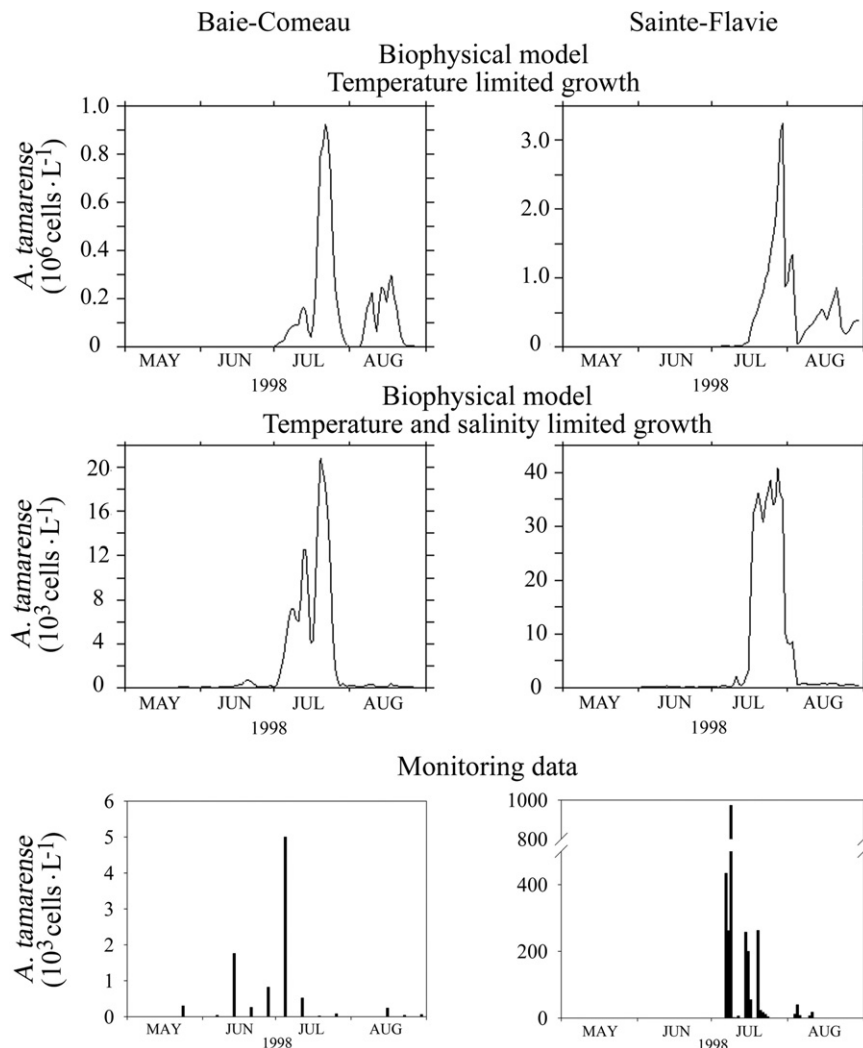

Fig. 6. Temporal evolution of simulated and observed *A. tamarense* concentrations at the monitoring stations of Baie-Comeau on the north shore and Sainte-Flavie on the south shore.

1998 is presented in Fig. 6. Results of the coupled model, with the salinity limitation of growth (Fig. 6), compare well with the observations at both monitoring stations (Fig. 6). The simulated timing of the bloom is consistent with observations. The simulated bloom developed in May and June and peaked in July as observed at the monitoring stations, although a few days later. Simulated *A. tamarense* cell concentrations at the Baie-Comeau station are consistent with the observations during the period of development of the bloom: the simulated concentrations (with salinity and temperature limitation of growth) reached 1000 cells L^{-1} on 19 June compared to mid-June in the observations and they peaked at around 6000 cells L^{-1} at the beginning of July compared to 5000 cells L^{-1} in the observations. However, at this station, the model generated higher *A. tamarense* concentrations later in July while observed concentrations decreased. At the Sainte-Flavie station, the simulated results never reached the high concentrations measured at the beginning of July when the red tide was detected. The model did not capture the first peak in *A. tamarense* concentrations at this station, which occurred between 7 and 9 July (Fig. 6). Still, the decline of the bloom in August is reproduced at both stations. The comparison between simulations with and without the salinity limitation of growth shows that this growth limitation by high salinity was responsible for the absence of bloom in August in the simulations. Therefore, our results suggest that the salinity limitation of *A. tamarense* growth affects the temporal evolution of the simulated bloom inside the plume (Fig. 6) but not its spatial distribution in the LSLE (Fig. 5).

In Fig. 7, we compare the timing of the retention–advection cycles of the M-O freshwater plume determined from the simulation results with the *A. tamarense* concentrations measured at the monitoring stations during the summer 1998 (Baie-Comeau on the north shore and Sainte-Flavie on the south shore, see Fig. 3 for the location of these stations) and, also, with measured salinity at Sainte-Flavie. The observed increases in *A. tamarense* abundance at the north shore station always occurred during periods of retention of the freshwater plume, while observed increases in *A. tamarense* abundance at the south shore station occurred during periods of advection of the plume. In particular, the detection of the *A. tamarense* red tide at the south shore station in 1998 (up to 9.7×10^5 cells L^{-1} on 9 July, see Fauchot et al., 2005a for more details) coincided with the simulated advection of the M-O plume toward the south shore after several days of retention on the north shore. Except during May when salinity at the Sainte-Flavie
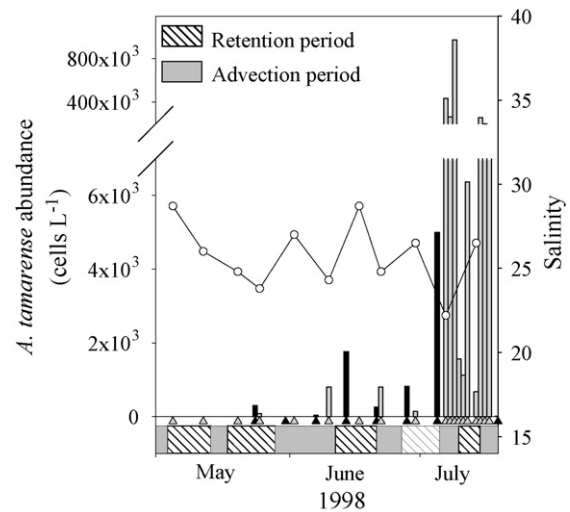

Fig. 7. Temporal evolution, from 1st May to 20 July 1998, of observed *A. tamarense* abundance at the monitoring stations of Baie-Comeau (north shore, black bars) and Sainte Flavie (south shore, grey bars), observed salinity at Sainte-Flavie (open circles) and periods of retention toward the north shore and advection toward the south shore of the M-O freshwater plume determined from the model simulation. The sampling dates at the Baie-Comeau and Sainte-Flavie monitoring stations are indicated by black and grey triangles, respectively.

monitoring station was probably mostly influenced by the end of the spring freshet, simulated periods of retention of the M-O plume coincided with measured increases in salinity on the south shore, while simulated periods of advection coincided with the lowest salinities recorded at Sainte-Flavie. These observations show that the retention–advection cycles of the M-O plume are representative of the conditions in the LSLE during the summer 1998.

Comparison of the spatial distribution of the simulated bloom with observations is presented in Fig. 8, for the days in July when *A. tamarense* concentrations were available in the estuary. The model generated a region of higher cell concentrations along the south shore on 9 July, with decreasing concentrations toward the north as measured. However, the simulated bloom was located more downstream in the estuary (ca. 20 km) compared with the observations (Fig. 8a and c). The simulated M-O plume and the associated bloom did not reach the Sainte-Flavie monitoring station on 9 July. This is in contradiction with the observations at the Sainte-Flavie monitoring station, which show a sharp decrease in salinity, associated with an increase in *A. tamarense* concentration between 7 and 9 July (Fig. 7). The spatial distribution of the plume and the associated bloom along the south shore are thus not precisely reproduced.
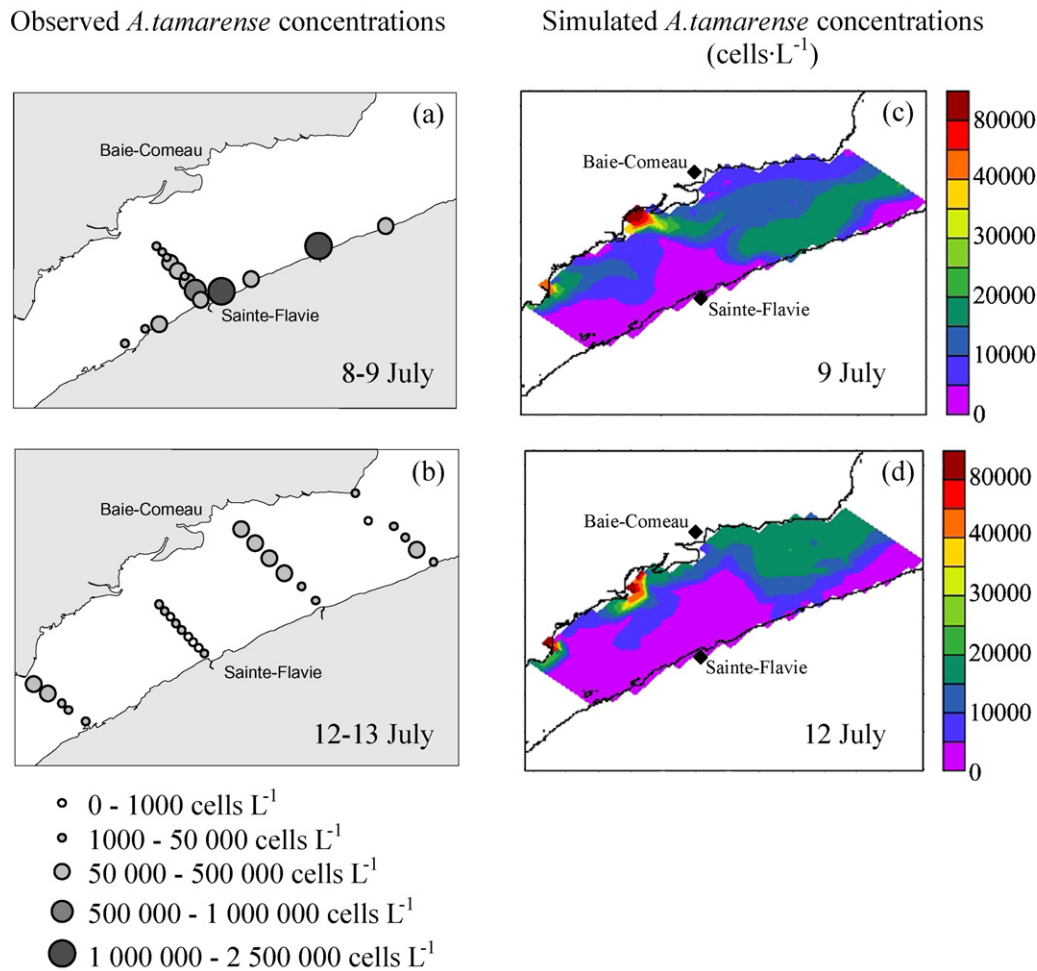
Observed *A.tamarense* concentrations

Simulated *A.tamarense* concentrations
(cells·L^{-1})

○ 0 - 1000 cells L^{-1}

○ 1000 - 50 000 cells L^{-1}

○ 50 000 - 500 000 cells L^{-1}

● 500 000 - 1 000 000 cells L^{-1}

● 1 000 000 - 2 500 000 cells L^{-1}

Fig. 8. Observed (a and b) and simulated (c and d) spatial distribution of the *A. tamarense* bloom in the surface layer in the LSLE on 2 days during the peak of the bloom, 9 and 12 July.

This explains why the model does not capture the first peak concentration of *A. tamarense* at the Sainte-Flavie station (Fig. 6). However, the general distribution of the bloom is reproduced rather well since, 3 days later, the model generated higher concentrations in the northern part of the estuary in agreement with the observations (Fig. 8b and d). As noted before, the absolute values of cell abundance and the decrease in cell abundance between 9 and 12 July are not well reproduced by the model.

4. Discussion

4.1. Ability of the coupled model to reproduce the A. tamarense bloom during the summer 1998

The coupled model generates a realistic timing of the *A. tamarense* bloom, with a development period in May and June, a peak in July and a decrease in August. These results are consistent with previous observation in the LSLE (Blasco et al., 2003) and with the results from two monitoring stations in the estuary during the 1998 summer. The ability of the model to reproduce the timing of the bloom results from the temperature and salinity limitations of the growth rate which define the temporal window in which the bloom can develop. During their modeling study, Yamamoto and Seike (2003) also found that temperature and salinity influence the timing of *A. tamarense* blooms in Hiroshima Bay (Japan). Spatially, the model reproduces the coincidence of the bloom with the M-O freshwater plume, a well-known characteristic of *A. tamarense* blooms in the LSLE (Therriault et al., 1985; Therriault and Levasseur, 1986; Cembella and Therriault, 1989). In addition, the model reproduces the variations in the north-south gradients in *A. tamarense* concentrations as

a result of the wind-driven retention–advection cycles of the M-O plume. However, the model is less efficient in reproducing the west-east gradients linked to the spatial extent of the plume. Consequently, for the simulation period, the model can predict when the bloom develops on the north shore and when it reaches the south shore, but fails to indicate precisely where the bloom will be delivered on the south shore. This problem might result from the resolution of the circulation model that is half to one third of the baroclinic Rossby radius of deformation (10–15 km) in the LSLE and Gulf of St. Lawrence. The model is able to generate mesoscale features but may not allow a precise reproduction of the extent of the M-O plume.

A. tamarense cell concentrations are not accurately simulated by the coupled model. This probably reflects the empirical and rather simple formulation of the biological model. This first version of the model takes into account a limited number of parameters for which we had information: cyst germination dynamics, and salinity and temperature limitation of cellular growth. The excessive cell concentrations generated in July at the Baie-Comeau station on the north shore highlight the need to regulate *A. tamarense* growth (e.g., by phosphate as suggested by Fauchot et al., 2005a,b) and to include loss terms (e.g., grazing, encystment). In contrast, the inability of the model to reproduce the red tide concentrations reached in 1998 on the south shore indicates first that physical accumulation alone, as simulated by the 5-km resolution circulation model, was apparently not responsible for these red tide concentrations and, second, that the model may be missing important biological processes leading to the accumulation of vegetative cells. The variability of the observed growth rates during the red tide (0.20–0.55 day^{-1}, Fauchot et al., 2005a) stresses the importance of developing in the model a parameterization of the growth function with a variable growth rate. The ability of *A. tamarense* to perform vertical migration, a behavior not considered in the model, could also explain the mismatch between the observed and the simulated concentrations. During their study in the LSLE, Fauchot et al. (2005b) reported rapid cell aggregations close to the surface in the morning and during the night leading to fast population growth rates. Since most of our sampling was conducted during daytime and in surface water, we hypothesize that the very high cell concentrations observed during the red tide resulted partly from their active aggregation close to the surface. This hypothesis is supported by two observations: (1) the appearance of these high abundances was preceded by several days of calm

winds, conditions favoring aggregation; (2) a sudden decrease in concentrations was recorded a few days later (on 12 July) after 2 days of high winds (Fauchot et al., 2005a). In summary, the timing and spatial distribution of *A. tamarense* bloom generated by the model are in general agreement with the summer 1998 observations. However, including a dynamical parameterization of the growth function, vertical migrations and loss processes in the biological model would, along with an increased resolution of the circulation model, probably improve the ability of the model to reproduce more accurately *A. tamarense* concentrations and spatial distribution during blooms in the LSLE.

4.2. Preferential inoculation of the M-O plume region

The results of the model show a preferential inoculation of the waters located along the north shore, especially in the region influenced by the M-O freshwater plume. A closer look at the model results suggests that this reflects the interaction between the simulated *A. tamarense* cyst dynamics and water circulation in the different layers of the LSLE. Along the south shore, most newly germinated cells are advected out of the studied area before reaching the surface layer. They are either advected upstream within the Laurentian channel (layers ≥ 100 m) or advected downstream along the Gaspé Peninsula (especially at depths above 50 m). In contrast, the newly germinated cells along the north shore are less affected by advection during their ascension in the water column and inoculate more efficiently the surface layer. Cembella et al. (1988) and Turgeon et al. (1990) measured high concentrations of cysts along the north shore and hypothesized that this region was acting as a benthic cyst reservoir for the initiation of *A. tamarense* blooms in the LSLE. Our results show that the importance of this local cyst bed also results from the particular circulation that tends to retain the newly germinated cells in the river plume. During the simulation period, once inoculated in the surface waters of the M-O plume, the *A. tamarense* cells remain and develop in the plume. A similar retention mechanism involving a localized cyst bed and a river plume has been suggested to explain the dynamics of *Alexandrium fundyense* blooms in the Gulf of Maine (McGillicuddy et al., 2003). The preferential inoculation of the M-O plume region is an important finding in regards to previous studies showing that the conditions present in the M-O plume stimulated the growth of *A. tamarense* (Fauchot et al., 2005a; Gagnon et al., 2005). Our results clearly show

that the coincidence of *A. tamarense* blooms with the plume in 1998 resulted mostly from this preferential inoculation of the M-O plume close to the north shore.

4.3. Importance of the M-O plume dynamics for the spatio-temporal distribution of the bloom

The model generates an *A. tamarense* bloom within the M-O freshwater plume, along the north shore. Previous studies already showed that, during the summer months, the M-O plume gains considerably in importance in the LSLE and that it has a strong influence on the spatial distribution of phytoplankton, and especially dinoflagellates (Therriault et al., 1985; Therriault and Levasseur, 1986). Our model confirms that *A. tamarense* blooms developing close to the north shore are transported across the estuary by the M-O plume and delivered to the south shore as previously suggested by Larocque and Cembella (1990) and Turgeon et al. (1990). The simulation results reveal that alternating periods of retention and advection of the M-O plume dominate the spatio-temporal evolution of the bloom: east or northeast winds result in the retention of the plume close to the north shore, while west or north-west winds result in its advection toward the south shore. Such a relationship between wind-driven freshwater plume dynamics and the delivery of *Alexandrium* populations to the shore has also been observed in the Gulf of Maine. *A. fundyense* populations are associated with a buoyant plume derived from river outflows in western Gulf of Maine. As observed in the St. Lawrence, the blooms are delivered to the coast, along with the freshwater plume, during downwelling-favorable wind events (Anderson et al., 2005; Keafer et al., 2005). Furthermore, a modeling study also suggests that the initiation of coastal blooms of *A. fundyense* from cysts located in offshore sediments in the Gulf of Maine could be the result of the transport of newly germinated *A. fundyense* cells within the freshwater plume, under favorable wind conditions (McGillicuddy et al., 2003).

The retention–advection cycles generated by the model present strong similarities with wind-driven circulation patterns previously reported for the LSLE (El-Sabh, 1979; Mertz et al., 1988; Koutitonsky and Bugden, 1991), especially with the two summer configurations identified by Mertz et al. (1989) and Koutitonsky et al. (1990). The first one, called the "high runoff basic state" by Koutitonsky et al. (1990), is characterized by strong seaward flow along the north shore of the estuary, an anti-cyclonic eddy in the downstream part of the estuary with a transverse front at the mouth that drives the outflow of estuarine waters to the south. This configuration is similar to the simulated M-O plume advection pattern. The second configuration is characterized by strong inflow along the north shore, weak outflow along the south shore and a cyclonic eddy near the mouth of the estuary. This reverse circulation, which can result from high-frequency events such as strong winds blowing from the Gulf toward the Estuary (Koutitonsky et al., 1990), is consistent with the simulated M-O plume retention pattern.

With an *in situ* growth rate probably never exceeding 0.55 day^{-1} (Levasseur et al., 1995; Parkhill and Cembella, 1999; Fauchot et al., 2005a), the retention of the plume along the north shore during several days may represent an essential pre-requisite for the development of *A. tamarense* blooms in the LSLE. Based on our simulations, the circulation was mostly in a retention mode in 1998 with more days of retention than days of advection of the M-O plume between May 1st and July 20. These results suggest that the residence time of the M-O plume and associated *A. tamarense* population in the LSLE was important during the summer 1998 and that it probably contributed to the development of the red tide. *A. tamarense* blooms development is also probably affected by the wind regime through its influence on turbulence which, in turn, determines whether or not *A. tamarense* cells can perform vertical migrations and aggregate at the depth of their optimal light intensity during the day or access the deep nitrate pool at night (Fauchot et al., 2005b). Therefore, we hypothesize that the wind-driven dynamics of the M-O plume could partly determine the success of *A. tamarense* blooms in the LSLE by influencing both the residence time of the blooms and the stability of the water column. This hypothesis is in agreement with Therriault et al. (1985) who stated that variations in the wind regime could explain the interannual variations in shellfish toxicity in the St. Lawrence estuary. On the other hand, Eilertsen and Wyatt (1998) concluded from a long-term (20 years) modeling study of *Alexandrium* bloom dynamics on the northeast coast of England that variations in hydrological and meteorological conditions were less important regulators of bloom success than cyst bed dynamics. The dynamic of cyst reservoirs should, thus, not be neglected in future studies on the interannual variability of *A. tamarense* blooms in the LSLE.

5. Conclusion

The timing of the *A. tamarense* bloom, its coincidence with the M-O freshwater plume and the

temporal variations in the north-south gradients in cell concentrations generated by the coupled model are in general agreement with field observations. Some improvements are needed to better reproduce the west-east gradients in cell distribution and the maximum concentrations reached during the bloom. The simulation results reveal that a preferential inoculation of the surface waters of the M-O river plume along the north shore partly explains the coincidence of blooms with the freshwater plume. Furthermore, our results suggest that the spatio-temporal evolution of the bloom is dominated by the retention–advection cycles of the M-O plume, which control the delivery of the *A. tamarense* populations from the northern part of the estuary to the south shore. These wind-driven dynamics of the M-O plume could influence the success of the blooms, by affecting the water column stability, and thus *A. tamarense* growth, and the residence time of the blooms. Further investigations are required to determine if variations in the wind regime, and the associated M-O plume dynamics, can account for the important interannual variability of *A. tamarense* blooms in the LSLE.

Acknowledgements

References

Anderson, D.M., Keafer, B.A., Geyer, W.R., Signell, R.P., Loder, T.C., 2005. Toxic *Alexandrium* blooms in the western Gulf of Maine: The plume advection hypothesis revisited. Limnol. Oceanogr. 50, 328–345.

Blasco, D., Levasseur, M., Bonneau, E., Gélinas, R., Packard, T.T., 2003. Patterns of paralytic shellfish toxicity in the St. Lawrence region in relationship with the abundance and distribution of *Alexandrium tamarense*. Sci. Mar. 67, 261–278.

Cembella, A.D., Turgeon, J., Therriault, J.-C., Béland, P., 1988. Spatial distribution of *Protogonyaulax tamarensis* resting cysts in nearshore sediments along the north coast of the lower St. Lawrence estuary. J. Shellfish Res. 7, 597–609.

Cembella, A.D., Therriault, J.C., 1989. Population dynamics and toxin composition of *Protogonyaulax tamarensis* from the St. Lawrence Estuary. In: Okaichi, T., Anderson, D.M., Nemoto, T. (Eds.), Red Tides: Biology, Environmental Science and Toxicology. Elsevier Publishers, New York, pp. 81–84.

Eilertsen, H.C., Wyatt, T., 1998. A model of *Alexandrium* population dynamics. In: Reguera, B., Blanco, J., Fernandez, M.L., Wyatt, T. (Eds.), Harmful Algae. Xunta de Galicia and Intergovernmental Oceanographic Commission of UNESCO, Vigo, pp. 196–199.

El-Sabh, M., 1979. The lower St. Lawrence estuary as a physical oceanographic system. Naturaliste Can. 106, 55–73.

Fauchot, J., Levasseur, M., Roy, S., Gagnon, R., Weise, A., 2005a. Environmental factors controlling *Alexandrium tamarense* (Dinophyceae) growth rate during a red tide event in the St. Lawrence estuary (Canada). J. Phycol. 41, 263–272.

Fauchot, J., Levasseur, M., Roy, S., 2005b. Daytime and nighttime vertical migrations of *Alexandrium tamarense* in the St. Lawrence estuary (Canada). Mar. Ecol. Prog. Ser. 296, 241–250.

Franks, P.J.S., Anderson, D.M., 1992. Alongshore transport of a toxic phytoplankton bloom in a buoyancy current: *Alexandrium tamarense* in the Gulf of Maine. Mar. Biol. 116, 153–164.

Gagnon, R., Levasseur, M., Weise, A.M., Fauchot, J., Campbell, P.G.C., Vigneault, B., Weissenboeck, B., Merzouk, A., Gosselin, M., 2005. Growth stimulation of *Alexandrium tamarense* (Dinophyceae) by humic substances from the Manicouagan river (Eastern Canada). J. Phycol. 41, 489–497.

Hunke, E.C., Dukowicz, J.K., 1997. An elastic-viscous-plastic model for sea ice dynamics. J. Phys. Oceanogr. 27, 1849–1867.

Ingram, R.G., El-Sabh, M.I., 1990. Fronts and mesoscale features in the St. Lawrence Estuary. In: El-Sabh, M.I., Silverberg, N. (Eds.), Oceanography of a Large-scale Estuarine System: The St. Lawrence. Springer-Verlag, New York, pp. 71–93.

Keafer, B.A., Churchill, J.H., McGillicuddy, D.J., Anderson, D.M., 2005. Bloom development and transport of toxic *Alexandrium fundyense* populations within a coastal plume in the Gulf of Maine. Deep-Sea Res. 52, 2674–2697.

Koutitonsky, V.G., Wilson, R.E., El-Sabh, M.I., 1990. On the seasonal response of the lower St. Lawrence estuary to buoyancy forcing by regulated river runoff. Estuar. Coast. Shelf Sci. 31, 359–379.

Koutitonsky, V.G., Bugden, G.L., 1991. The physical oceanography of the Gulf of St. Lawrence: a review with emphasis on the synoptic variability of the motion. In: Therriault, J.-C. (Ed.), The Gulf of St. Lawrence: Small Ocean or Big Estuary? Can. Spec. Publ. Fish. Aquat. Sci. 113, 57–90.

Larocque, R., Cembella, A.D., 1990. Ecological parameters associated with the seasonal occurrence of *Alexandrium* spp. and consequent shellfish toxicity in the lower St. Lawrence estuary (eastern Canada). In: Granéli, E., Sundström, B., Edler, L., Anderson, D.M. (Eds.), Toxic Marine Phytoplankton. Elsevier Science Publishing Co., Inc., New York, pp. 368–373.

Le Fouest, V., Zakardjian, B., Saucier, F.J., Çizmeli, S.A., 2006. Application of SeaWIFS- and AVHRR-derived data for mesoscale and regional validation of 3-D high-resolution

physical–biological model of the Gulf of St. Lawrence (Canada). J. Mar. Syst. 60, 30–50.

Levasseur, M., Gamache, T., Saint-Pierre, I., Michaud, S., 1995. Does the cost of NO_3^- reduction affect the production of harmful compounds by *Alexandrium excavatum*? In: Lassus, P., Arzul, G., Erard, E., Gentien, P., Marcaillou, C. (Eds.), Harmful Marine Algal Blooms. Lavoisier, Intercept Ltd., Paris, pp. 463–468.

MacIntyre, J.G., Cullen, J.J., Cembella, A.D., 1997. Vertical migration, nutrition and toxicity in the dinoflagellate *Alexandrium tamarense*. Mar. Ecol. Prog. Ser. 148, 201–216.

McGillicuddy, D.J., Signell, R.P., Stock, C.A., Keafer, M.D., Keller, M.D., Hetland, R.D., Anderson, D.M., 2003. A mechanism for offshore initiation of harmful algal blooms in the coastal Gulf of Maine. J. Plankton Res. 25, 1131–1138.

Mertz, G., El-Sabh, M.I., Koutitonsky, V.G., 1988. Wind-driven motions at the mouth of the lower St. Lawrence estuary. Atmos. Ocean 26, 509–523.

Mertz, G., El-Sabh, M.I., Koutitonsky, V.G., 1989. Low frequency variability in the lower St. Lawrence estuary. J. Mar. Res. 47, 285–302.

Parkhill, J.-P., Cembella, A.D., 1999. Effects of salinity, light and inorganic nitrogen on growth and toxigenicity of the marine dinoflagellate *Alexandrium tamarense* from northeastern Canada. J. Plankton Res. 21, 939–955.

Perez, C.C., Roy, S., Levasseur, M., Anderson, D.M., 1998. Control of germination of *Alexandrium tamarense* (Dinophyceae) cysts from the lower St. Lawrence estuary (Canada). J. Phycol. 34, 242–249.

Prakash, A., 1967. Growth and toxicity of a marine dinoflagellate, *Gonyaulax tamarensis*. J. Fish. Res. Bd. Canada 24, 1589–1606.

Saucier, F.J., Roy, F., Gilbert, D., Pellerin, P., Ritchie, H., 2003. Modeling the formation and circulation processes of water masses and sea ice in the Gulf of St. Lawrence, Canada. J. Geophys. Res. 108, 1–20.

Saucier, F.J., Senneville, S., Prinsenberg, S., Roy, F., Gachon, P., Caya, D., Laprise, R., 2004. Modeling the ice-ocean seasonal cycle in Hudson Bay, Foxe Basin and Hudson Strait. Canada Clim. Dyn. 23, 303–326.

Semtner Jr., A.J., 1976. A model for the thermodynamic growth of sea ice in numerical investigations of climate. J. Phys. Oceanogr. 6, 379–389.

Therriault, J.-C., Painchaud, J., Levasseur, M., 1985. Factors controlling the occurrence of *Protogonyaulax tamarensis* and shellfish toxicity in the St. Lawrence Estuary: freshwater runoff and the stability of the water column. In: Anderson, D.M., White, A.W., Baden, D.G. (Eds.), Toxic Dinoflagellates. Elsevier Science Publishing Co., New York, pp. 141–146.

Therriault, J.C., Levasseur, M., 1986. Freshwater runoff control of the spatio-temporal distribution of phytoplankton in the lower St. Lawrence estuary. In: Skreslet, S. (Ed.), The Role of Freshwater Outflow in Coastal Marine Ecosystems. Springer-Verlag, Berlin, pp. 251–260.

Turgeon, J., Cembella, A.D., Therriault, J.C., Beland, P., 1990. Spatial distribution of resting cysts of *Alexandrium* spp. in sediments of the lower St. Lawrence estuary and the Gaspé coast (eastern Canada). In: Graneli, E., Sundstroem, B., Edler, L., Anderson, D.M. (Eds.), Toxic Marine Phytoplankton. Elsevier Science Publishing Co., Inc., pp. 238–243.

Vézina, A.F., Gratton, Y., Vinet, P., 1995. Mesoscale physical–biological variability during a summer phytoplankton bloom in the lower St. Lawrence estuary. Estuar. Coast. Shelf Sci. 41, 393–411.

Yamamoto, T., Seike, T., 2003. Modelling the population dynamics of the toxic dinoflagellate *Alexandrium tamarense* in Hiroshima Bay, Japan. II. Sensitivity to physical and biological parameters. J. Plankton Res. 25, 63–81.